

Optimal Planar Evasive Aircraft Maneuvers Against Proportional Navigation Missiles

Shaw Y. Ong*

Singapore Technologies Aerospace, Ltd., Paya Lebar 1953, Singapore
and

Bion L. Pierson†

Iowa State University, Ames, Iowa 50011-3231

A comparative study of evasive strategies of an aircraft against a missile with fixed, gravity-limited, proportional navigation is conducted for both subsonic and supersonic confrontations. A complete point-mass aircraft model and a variable-mass missile model that includes missile dynamics are used. No linearization is required in the analysis, and all motion is constrained to a horizontal plane. Sequential quadratic programming is used to solve the optimal control problem. Numerical results are presented for an early model of the F-4 fighter aircraft. In particular, the effects of varying the aircraft/missile initial velocity ratio, the missile initial heading angle, and the missile guidance time constant are determined.

Introduction

MISSILE-EVASION problems have been treated by many investigators.^{1–10} A good example of a nonlinear differential game analysis for fixed-speed vehicles can be found in the literature.¹ Fixing the missile navigation strategy and forming a one-sided optimal control problem for the evader has become the latest approach to treating this problem. Because optimal control problems generally are less complicated than their differential game counterparts, the optimal control formulation allows one to use more realistic models for the evading aircraft dynamics. Julich and Borg² worked with the missile-evasion problem posed as an optimal control problem, but they assume constant speeds for both the aircraft and the missile. Slater and Wells³ studied evasive tactics that involve linearized kinematics and a time delay. Shinar and Steinberg,⁴ Shinar et al.,⁵ and Ben-Asher et al.^{6,7} also investigated evasive maneuvers by assuming linearized kinematics with constant speeds. These assumptions, however, often result in limited applicability; in particular, they lead only to near head-on or tail-chase engagements. This is not true in a general situation, as shown by Forte et al.⁸ in a study of the effects of nonlinear kinematics in optimal evasion. Guelman and Shinar⁹ obtain a closed-form optimal guidance law for the pursuing missile, assuming constant missile and aircraft speeds and complete knowledge of the aircraft motion. A more complete model for the aircraft evasion problem is presented by Imado and Miwa.¹⁰ Their dynamic models are similar to those used here except for the variable-mass feature and the numerical method used.

We study optimal open-loop evasive strategies of an aircraft being pursued by a missile with a fixed-structure, proportional-navigation^{11,12} guidance system that is gravity-limited. The entire maneuver takes place in a horizontal plane. Simplified nonlinear missile dynamics are assumed. No linearization is employed. Also, instead of a simplified aircraft dynamic model, we are using a complete two-dimensional, point-mass aircraft model with realistic aerodynamic forces and thrust characteristics. And unlike previous work, we are treating the optimal control problem as an approximate parameter optimization problem, i.e., we will choose a form for the control function that contains a finite number of parameters, and

then minimize the performance index over this set of parameters. The resulting parameterized optimal control problem is more flexible and easier to solve. The numerical results presented here are for an early representation of the F-4 fighter aircraft.

System Models

Figure 1 shows the relative geometry for the missile-evasion problem. The subscript *m* is used to denote the missile, and a subscript *e* denotes the evader aircraft. The model used is that of a point-mass vehicle flying over a flat, nonrotating earth. We consider only motion in the horizontal plane. The equations of motion used in our study are described below.

Evader Equations of Motion

The aircraft equations of motion form a fifth-order system: a standard fourth-order point-mass model plus a mass rate equation to account for fuel consumption. The governing equations are¹³

$$m_e \dot{V}_e = T_e \cos \alpha_e - D_e \quad (1)$$

$$m_e V_e \dot{\psi}_e = (T_e \sin \alpha_e + L_e) \sin \mu_e \quad (2)$$

$$\dot{x}_e = V_e \cos \psi_e \quad (3)$$

$$\dot{y}_e = V_e \sin \psi_e \quad (4)$$

$$\dot{m}_e = -(T_e/cg) \quad (5)$$

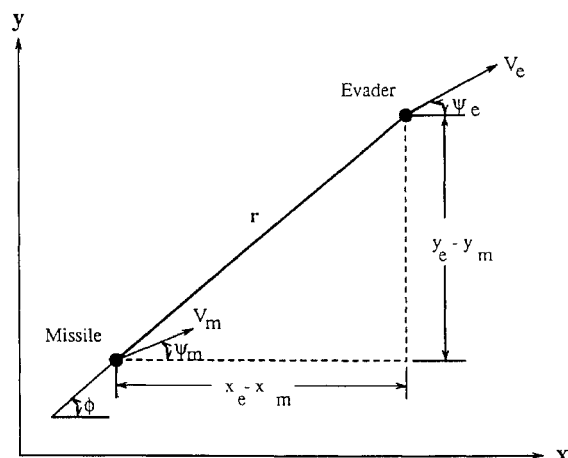


Fig. 1 Nomenclature and interception geometry.

Received June 7, 1995; revision received April 26, 1996; accepted for publication June 19, 1996. Copyright © 1996 by the American Institute of Aeronautics and Astronautics, Inc. All rights reserved.

*Senior Engineer, Engineering Development Centre, 540 Airport Road, Member AIAA.

†Professor, Department of Aerospace Engineering and Engineering Mechanics, Associate Fellow AIAA.

where V_e , ψ_e , x_e , y_e , and m_e are the velocity, heading angle, down range, cross range, and mass of the evader, respectively. The bank angle μ_e is the control. The aerodynamic forces, lift L_e and drag D_e , are given by¹⁴

$$L_e = qSC_L = qSC_{L\alpha}\alpha_e \quad (6)$$

$$D_e = qSC_D = qS(C_{D0} + \eta C_{L\alpha}\alpha_e^2) \quad (7)$$

where $q = \frac{1}{2}\rho(h)V_e^2$ is the dynamic pressure. T_e is the maximum thrust; it depends on speed V_e and the specified altitude h . The angle of attack α_e is determined via the constant-altitude constraint. If we set $\dot{\gamma} = 0$, where γ is the flight-path angle, the flight-path angle dynamics yield

$$(T_e \sin \alpha_e + L_e) \cos \mu_e = m_e g \quad (8)$$

Assuming small α_e , we get

$$\alpha_e = \frac{m_e g}{(T_e + qSC_{L\alpha}) \cos \mu_e} \quad (9)$$

This relation is used both in the equations of motion (1) and (2) and in the aerodynamic forces (6) and (7). Also, our solution method provides a mechanism for bounding the angle of attack on a point-by-point basis should α_{stall} be exceeded. However, from the results we have obtained, this bound is not necessary. The specific fuel consumption, $1/c$, is assumed to be constant. The aerodynamic coefficients C_{D0} , η , and $C_{L\alpha}$ are all specified functions of Mach number, $M = V_e/a(h)$, where $a(h)$ is the local speed of sound.

Missile Equations of Motion

Our missile dynamic model consists of modified, variable point-mass, translational equations for flight in the horizontal plane. The missile heading angle rate is assumed to depend on its guidance command instead of the usual missile aerodynamic and thrust characteristics.² These equations of motion result in a fifth-order dynamic system:

$$m_m \dot{V}_m = T_m - D_m \quad (10)$$

$$\dot{\psi}_m = U_m \quad (11)$$

$$\dot{x}_m = V_m \cos \psi_m \quad (12)$$

$$\dot{y}_m = V_m \sin \psi_m \quad (13)$$

$$\dot{U}_m = \frac{1}{\tau_m} U_{m\max} \frac{2}{\pi} \tan^{-1} \left(\frac{\sqrt{3} n \dot{\phi}}{U_{m\max}} \right) - \frac{1}{\tau_m} U_m \quad (14)$$

Here, V_m , ψ_m , x_m , y_m , and U_m are the velocity, heading angle, down range, cross range, and missile guidance heading rate, respectively. Equation (14) is the guidance dynamics,² where n is the navigation constant and τ_m is the time constant. The arctangent function is chosen to ensure that the missile's guidance heading rate does not approach infinity for large line-of-sight (LOS) rotation rates, particularly toward the end of the confrontation. The maximum missile guidance heading rate, $U_{m\max}$, is gravity-limited and is given by

$$U_{m\max} = \frac{g G_{m\max}}{V_{m\text{const}}} \quad (15)$$

where $G_{m\max}$ is the maximum gravity loading and $V_{m\text{const}}$ is 2000 ft/s. The LOS rotation rate $\dot{\phi}$ is

$$\dot{\phi} = \frac{\Delta y \Delta x - \Delta y \dot{\Delta} x}{r^2} \quad (16)$$

where $\Delta x = x_e - x_m$ and $\Delta y = y_e - y_m$. The relative distance $r(t)$ at any time is $r^2(t) = \Delta x^2(t) + \Delta y^2(t)$. The missile thrust T_m , drag D_m , and variable mass m_m are given, respectively, by¹⁰

$$T_m(t) = \begin{cases} T_{\max}, & 0 \leq t \leq t_m \\ 0, & t_m < t \end{cases} \quad (17)$$

Table 1 Model parameters

Evader	Missile
$c = 1600 \text{ s}$	$n = 3$
$S = 530 \text{ ft}^2$	$t_m = 10 \text{ s}$
	$\tau_m = 0.5 \text{ s}$
	$T_{\max} = 1350.0 \text{ lb}$
	$m_m = 13.71 \text{ slugs}$
	$a_1 = 1.0717(10^{-4}) \text{ slugs/ft}$
	$a_2 = 4.745(10^4) \text{ slug-ft}$
	$G_{m\max} = 10$
	$V_{m\text{const}} = 2000 \text{ ft/s}$

$$D_m = a_1 V_m^2 + a_2 \dot{\psi}_m^2 \quad (18)$$

$$m_m(t) = \begin{cases} -0.8226t + 13.71, & 0 \leq t \leq t_m \\ 5.484, & t_m < t \end{cases} \quad (19)$$

where the parameter values are shown in Table 1. Note that the missile is assumed to lose 60% of its initial mass as its propellant is burned.

Problem Statement

The objective of this study is to maximize the relative distance $r(t_f)$ at the time of closest approach t_f . Thus, the missile-evasion problem can be stated as follows.

Find the evader bank-angle history, $\mu_e(t)$, that minimizes

$$J = -r^2(t_f) \quad (20)$$

subject to the evader state equations (1–5), the missile state equations (10–14), the specified initial states, and the control constraint

$$-85 \text{ deg} \leq \mu_e(t) \leq 85 \text{ deg} \quad (21)$$

The terminal time t_f , when the missile has come closest to the evader, is determined by setting the LOS relative velocity to zero:

$$\dot{r} = \frac{\dot{\Delta} x \Delta x + \Delta y \dot{\Delta} y}{r} = 0 \quad (22)$$

The terminal condition (22) can be interpreted as a zero scalar product between the relative position and velocity vectors.

Note that this is a moderately large nonlinear optimal control problem that involves bounded scalar control and a dynamic order of 10. Also, the problem is a variable end-time problem. The control bounds (21) have been chosen arbitrarily to prevent the singularity in Eq. (9) as bank angle approaches ± 90 deg.

Numerical Results

The above optimal control problem is converted to a nonlinear programming problem by approximating the control function (bank angle) by linear interpolation among a finite number of control points at fixed times and numerically integrating the resulting state equations. Sequential quadratic programming¹⁵ (SQP) then is used to solve the nonlinear programming problem. This method has proved to be very useful in solving other aircraft trajectory optimization problems.¹⁶ It can accommodate the desired dynamic model, state, and control constraint changes with relatively little reprogramming. The actual SQP algorithm used here is based on one of Poulitot.¹⁷ All related numerical computations were performed on a DEC 5000/125 workstation using Fortran 77 with double-precision arithmetic. A standard fourth-order, fixed-step, Runge–Kutta numerical integration scheme is used to integrate the differential constraints, and 200 integration steps are used to compute the trajectories presented here.

Because the missile evasion problem is a free end-time problem, we convert it to a fixed end-time problem via an additional control parameter, β , through the linear time transformation

$$t = \beta \tau, \quad 0 \leq \tau \leq \tau_{fn}, \quad 0 \leq t \leq t_f \quad (23)$$

Here, τ_{fn} is a fixed nominal final time. The i th state equation $dx_i/dt = f_i(x, u)$ is then transformed to $dx_i/d\tau = \beta f_i(x, u)$. The

Table 2 Initial flight conditions for control point studies

States	Evader flight condition		Missile flight condition	
	Initial state	Final state	Initial state	Final state
V	862.3 ft/s	free	1724.6 ft/s	free
ψ	0 deg	free	21.89 deg	free
x	11,200 ft	free	0	free
y	4500 ft	free	0	free
m	1088 slugs	free	13.71 slugs	free
U_m	no guidance		0	free

Table 3 CPU time comparisons with number of control points

Control points	CPU time/iteration, s
6	1.86
11	3.02
15	3.96
21	5.61

final time t_f thus becomes $\beta\tau_{fn}$, and the total number of design variables for the approximating nonlinear programming problem is equal to the number of control points plus one.

Data for the maximum thrust $T_e(V_e, h)$ and the aerodynamic coefficients are taken from an early representation of the F-4 fighter aircraft.¹⁴ We use analytical representations of these data prepared by Ong.¹⁸ The confrontation is assumed to occur at an altitude of 10,000 ft.

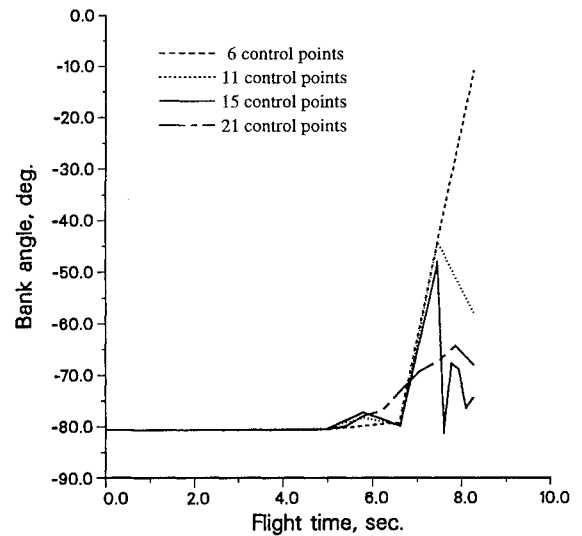
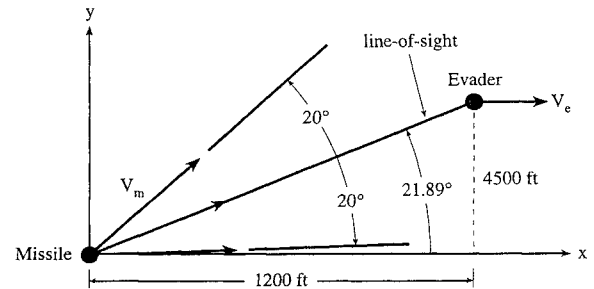
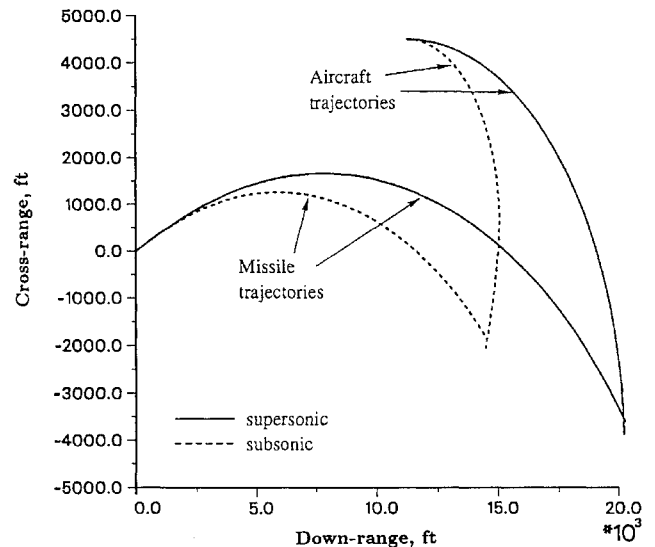
Choice of Control Points

Before proceeding to obtain optimal evasive strategies for a whole range of flight conditions, it is beneficial to determine first a reasonable number and distribution of control points to be used in all subsequent computations. For this study, the evader and missile model parameters and initial flight conditions are summarized in Tables 1 and 2, respectively. In Table 3, the CPU seconds per iteration computed for 6, 11, 15, and 21 control points are given. All control points are equally spaced except when 15 control points are used. In this case, the first 10 control points are equally distributed for the initial nine-tenths of the flight, whereas 5 are used for the last tenth. From Table 3, we note that computations with 21 control points cost approximately 3 times as much as those with 6 control points. The optimal bank-angle control histories for these control points are compared in Fig. 2. The results indicate nearly identical optimal bank-angle histories for the first 60% of the confrontation. This is attributable to the evasion being constrained to the horizontal plane and a maximum gravity-loading of 6. Near the end of the engagement, the bank-angle history becomes more oscillatory, and a higher density of control points is clearly desirable. In all cases, the miss distances and flight times are approximately the same (315 ft and 8.3 s, respectively), and the optimal evasion trajectories for the 15- and 21-point cases are virtually indistinguishable. From these comparisons, we have chosen to use 15 nonuniformly spaced control points as a reasonable compromise between simulation fidelity and computational effort. One advantage of using a direct SQP approach is that the number and location of the control points may be tailored to suit the specific problem under investigation.

Optimal Evasive Trajectories and Control Histories

In this section, we compute the optimal evasive maneuver for the aircraft against the missile for three different missile initial heading angles and four aircraft/missile initial velocity ratios (V_{e0}/V_{m0} of 0.5, 0.6, 0.7, and 0.8) for both subsonic and supersonic engagements. Figure 3 depicts the initial intercept geometry for the cases studied: missile initial heading angle at 20 deg to the left of the initial LOS, directly on the LOS, and 20 deg to the right of the LOS [$\psi_m(0) = 41.89, 21.89$, and 1.89 deg, respectively]. The initial Mach number of the evader is 0.8 (862.3 ft/s) for the subsonic engagement and 1.2 (1293.5 ft/s) for the supersonic engagement.

Although solutions for all of the above cases have been obtained, only the optimal evasive flight profiles for $\psi_m(0) = 21.89$ deg

**Fig. 2 Bank-angle history comparisons.****Fig. 3 Initial interception geometry.****Fig. 4 Optimal evasive flight profiles for aircraft subsonic and supersonic engagements (0 deg off LOS case, initial velocity ratio = 0.7).**

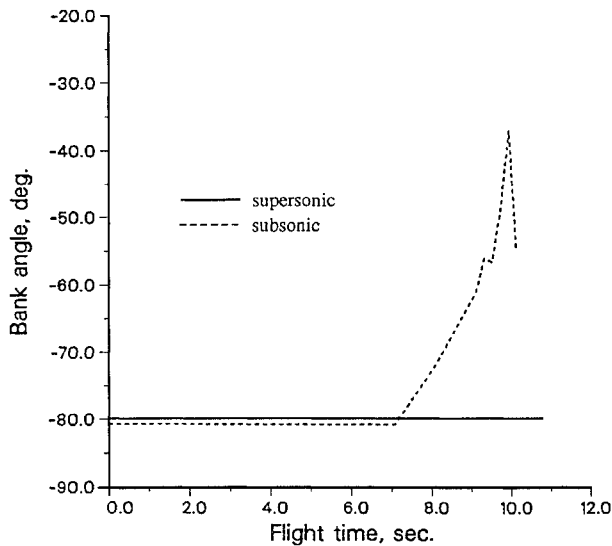
(directly on the LOS angle) and initial $V_{e0}/V_{m0} = 0.7$ are presented here. Figure 4 illustrates these optimal evasive flight profiles for both subsonic and supersonic aircraft confrontations [$\psi_e(0) = 0$ deg]. In both cases, the solutions show that turning initially toward the missile is optimal. In fact, this strategy is optimal for all initial geometries considered here. The turn radius for subsonic engagements, as expected, is smaller compared to those for supersonic engagements. In both cases, the missile point of closest approach is behind the aircraft. The aircraft reaches the intersection between the two trajectories before the missile, and the trajectory simulation ends at the instant of closest approach.

Table 4 Miss-distance and flight-time comparisons for various initial intercept geometries for subsonic confrontations ($M_e = 0.8$)

$V_e/V_m(0)$	+20 deg off LOS case		0 deg off LOS case		-20 deg off LOS case	
	Miss distance	Flight time	Miss distance	Flight time	Miss distance	Flight time
0.5	3969	9.3	315	8.3	1870	10.2
0.6	3894	10.9	293	9.5	2064	11.8
0.7	4073	12.0	202	10.1	2706	13.3
0.8	5073	13.0	228	11.0	3849	14.1

Table 5 Miss-distance and flight-time comparisons for various initial intercept geometries for supersonic confrontations ($M_e = 1.2$)

$V_e/V_m(0)$	+20 deg off LOS case		0 deg off LOS case		-20 deg off LOS case	
	Miss distance	Flight time	Miss distance	Flight time	Miss distance	Flight time
0.5	5330	7.6	434	7.4	479	9.0
0.6	5350	9.7	485	9.1	957	11.4
0.7	5025	12.1	276	10.8	1734	13.5
0.8	5374	14.6	635	11.8	3135	14.6

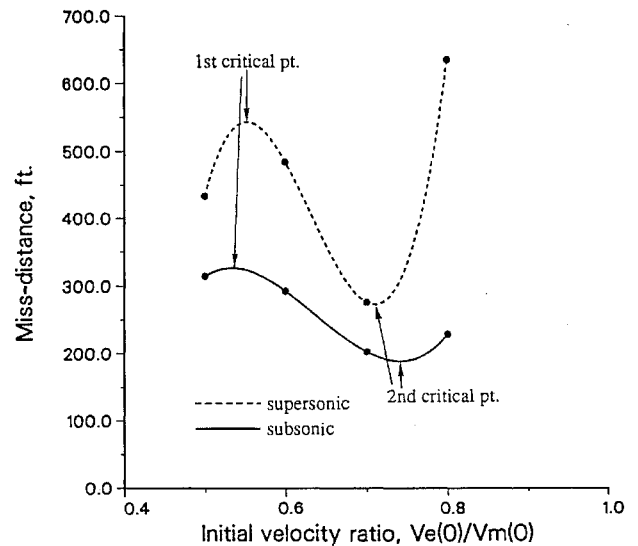
**Fig. 5** Optimal bank-angle control histories for aircraft subsonic and supersonic engagements (0 deg off LOS case, initial velocity ratio = 0.7).

The optimal bank-angle control histories for the above cases are shown in Fig. 5. For the subsonic engagement, the aircraft maintains a tight turn for the first two-thirds of the encounter, followed by a reduction in the bank angle and a corresponding increase in speed. At supersonic speeds, the less maneuverable aircraft maintains a tight turn for the entire encounter. In both cases, the lowest bank-angle value reached is approximately -80° (right turn). The $\pm 85^\circ$ bank-angle limits are not exceeded in either case. This is because the aircraft is constrained to only horizontal planar motion and may not exceed a normal acceleration of $6g$. As a result, bank-angle magnitudes greater than approximately 80° are not possible for these horizontal evasions.

We also have computed solutions using a constant-mass and constant-speed missile model. Although this model is unrealistic, we found that for low aircraft/missile velocity ratios, the optimal evasive maneuver is to turn toward the missile, whereas for high-velocity ratios, the optimal evasive maneuver is to turn away from or outrun the missile. In this paper, we employ a variable-mass missile model that includes missile dynamics. Thus, the speed of the missile increases rapidly, resulting in low instantaneous aircraft/missile velocity ratios throughout much of the confrontation. Because this ratio is small, the optimal evasive maneuver is to turn toward the missile, as obtained here.

Effect of Initial Missile Heading Angle and Aircraft/Missile Velocity Ratio

The results for this study are shown in Tables 4 and 5 for the cases mentioned above. From these tables, we note that the miss distances

**Fig. 6** Miss distance vs aircraft/missile initial velocity ratio for the 0 deg off LOS case.

for the $\pm 20^\circ$ off LOS cases are rather high, in the thousands of feet. These two cases are not a significant threat to the aircraft, at least in the subsonic case. In the 0 deg off LOS case, however, the aircraft is in serious danger of being hit. In general, the results are quite sensitive to initial missile heading angle, and this sensitivity changes as a function of initial evader speed and velocity ratio.

Figure 6 shows optimal miss distance plotted as a function of aircraft/missile initial velocity ratio for both subsonic and supersonic encounters. An important result can be seen. The relationship between miss distance and velocity ratio appears to be roughly sinusoidal. This leads to two critical initial velocity ratios. As the missile/aircraft initial velocity ratio increases from 0.5 up to the first critical value, the miss distance increases. This is because the aircraft begins to have a speed advantage and can outmaneuver the missile. After the first critical point, the miss distance begins to decrease. Here, the missile speed is low compared to that of the aircraft. (Recall that the aircraft initial speed is fixed, but the initial missile speed varies according to the respective initial velocity ratio.) Whatever evasive maneuvers are executed by the aircraft to increase the LOS rotation rate can be counteracted easily by the slower missile. This trend continues until the second critical initial velocity ratio is reached. Beyond this point, the miss distance increases because the aircraft now has a speed advantage over the missile and can simply outrun the missile for the optimal strategy.

These results lead to an important point. The miss distance does not always increase with missile/aircraft initial velocity ratio. In particular, there is an intermediate range of velocity ratio for which the miss distance decreases with increasing velocity ratio.

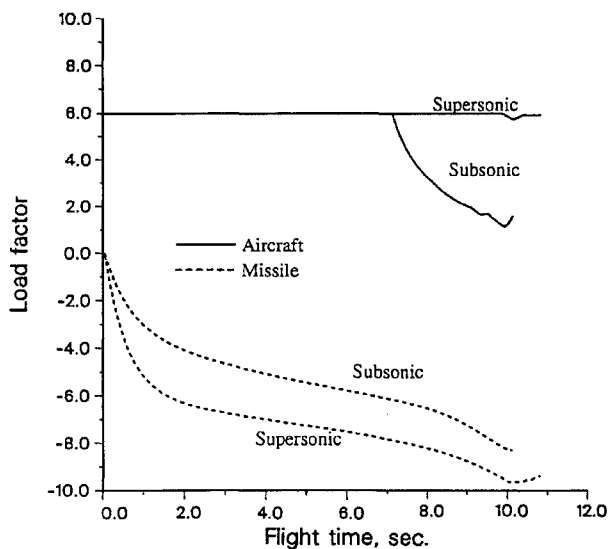


Fig. 7 Aircraft and missile load-factor histories for 0 deg off LOS subsonic and supersonic engagements with initial velocity ratio = 0.7.

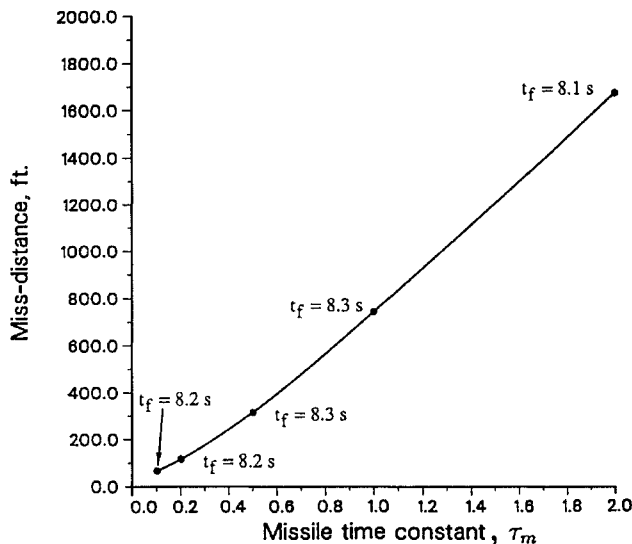


Fig. 8 Miss distance vs missile time constant for the 0 deg off LOS case and an initial velocity ratio of 0.5.

Load-Factor Histories

The aircraft and missile load-factor histories for 0 deg off LOS subsonic and supersonic speed engagements with an initial velocity ratio of 0.7 are given in Fig. 7. We note that the aircraft immediately sustains a maximum 6 g turn in its attempt to evade the missile. This continues throughout the entire encounter for the supersonic case, but not for subsonic engagements. In the latter case, the gravity loading decreases near the end of the confrontation.

The missile gravity loading, however, begins from zero and increases rapidly during the first second for both situations. This is because the missile is executing a very tight turn to counteract the high initial LOS rotation rate created by the aircraft evasive maneuver. Also, as expected, the magnitude of the missile gravity loading in the supersonic confrontation is higher than in the subsonic case, because turning at higher speeds results in larger load factors. After the first second, the increase in missile gravity loading is more gradual. For the initial interception geometry considered here, the gravity loading never reaches its saturation limit of 10. Although not shown here, when the initial relative distance between the aircraft and missile is sufficiently small, the missile does, of course, reach its saturation limit.

Effect of Missile-Guidance Time Constant

In Fig. 8, miss distance is plotted as a function of the missile time constant τ_m for the 0 deg off LOS case with a fixed initial velocity ratio of 0.5. It is clear that the miss distance becomes smaller as the missile time constant decreases. In this case, the miss distance appears to decrease linearly with missile time constant over much of the τ_m range. With $\tau_m = 2.0$, the miss distance is 1674 ft, but with $\tau_m = 0.2$, it is only 117 ft. For small missile time constant, the missile is able to react more quickly to the evasive strategies executed by the aircraft. The evasion flight time, however, seems not to be affected by the missile time constant.

Conclusions

In this paper, optimal aircraft evasive maneuvers against a proportional navigation missile are investigated for a horizontal planar engagement. We have worked with full point-mass aircraft dynamics, variable-mass missile dynamics, and acceleration constraints on both vehicles. The direct optimization procedure used here provides a flexible means of examining different confrontation configurations, flight conditions, and vehicle parameters.

Because a limited range of encounters have been treated here, we are reluctant to make general conclusions. However, several tentative conclusions are possible. For the missile initial-heading angles used here for both subsonic and supersonic confrontations, the optimal aircraft evasive maneuver is to turn toward the missile. The maximum miss distance depends strongly on both the initial velocity ratio and the initial missile-heading angle. For the solutions obtained here, both subsonic and supersonic aircraft optimal evasive strategies require maximum-gravity turns initially. But for the subsonic case, the aircraft reduces its gravity loading near the end of the confrontation and speeds up.

The miss distance between the aircraft and the missile at the terminal time does not always increase with aircraft/missile initial velocity ratio. Depending on the initial velocity ratio and the subsequent value of this ratio, the final miss distance can either increase or decrease.

Finally, the missile navigation time constant affects the optimal miss distance significantly. For the cases studied here, there appears to be a nearly linear relationship between these two quantities. However, the missile time constant does not substantially affect the evasion flight time.

References

- ¹Vincent, T. L., Sticht, D. J., and Peng, W. Y., "Aircraft Missile Avoidance," *Operations Research*, Vol. 24, No. 3, 1976, pp. 420-437.
- ²Julich, P. M., and Borg, D. A., "Proportional Navigation vs an Optimally Evading Constant-Speed Target in Two Dimensions," *Journal of Spacecraft and Rockets*, Vol. 7, No. 12, 1970, pp. 1454-1457.
- ³Slater, G. L., and Wells, W. R., "Optimal Evasive Tactics with Time Delay," *Journal of Spacecraft and Rockets*, Vol. 10, No. 5, 1973, pp. 309-313.
- ⁴Shinar, J., and Steinberg, D., "Analysis of Optimal Evasive Maneuvers Based on a Linearized Two-Dimensional Model," *Journal of Aircraft*, Vol. 14, No. 8, 1977, pp. 795-802.
- ⁵Shinar, J., Rosenzstein, Y., and Bezner, E., "Analysis of Three-Dimensional Optimal Evasion with Linearized Kinematics," *Journal of Guidance and Control*, Vol. 2, No. 5, 1979, pp. 353-360.
- ⁶Ben-Asher, J., Cliff, E. M., and Kelley, H. J., "Optimal Evasion with a Path-Angle Constraint and Against Two Pursuers," *Journal of Guidance, Control, and Dynamics*, Vol. 11, No. 4, 1988, pp. 300-304.
- ⁷Ben-Asher, J., and Cliff, E. M., "Optimal Evasion Against a Proportionally Guided Pursuer," *Journal of Guidance, Control, and Dynamics*, Vol. 12, No. 4, 1989, pp. 598-600.
- ⁸Forte, I., Steinberg, A., and Shinar, J., "Effects of Non-Linear Kinematics in Optimal Evasion," *Optimal Control Applications and Methods*, Vol. 4, No. 2, 1983, pp. 139-152.
- ⁹Guelman, M., and Shinar, J., "Optimal Guidance Law in the Plane," *Journal of Guidance, Control, and Dynamics*, Vol. 7, No. 4, 1984, pp. 471-476.
- ¹⁰Imado, F., and Miwa, S., "Fighter Evasive Maneuvers Against Proportional Navigation Missile," *Journal of Aircraft*, Vol. 23, No. 11, 1986, pp. 825-830.
- ¹¹Murtaugh, S. A., and Criel, H. E., "Fundamentals of Proportional Navigation," *Spectrum*, Vol. 3, No. 12, 1966, pp. 75-85.

¹²Zarchan, P., *Tactical and Strategic Missile Guidance*, AIAA, Washington, DC, 1990, Chap. 2.

¹³Miele, A., *Flight Mechanics, Vol. 1: Theory of Flight Paths*, Addison-Wesley, Reading, MA, 1962, Chap. 4.

¹⁴Bryson, A. E., Jr., Desai, M. N., and Hoffmann, W. C., "Energy-State Approximation in Performance Optimization of Supersonic Aircraft," *Journal of Aircraft*, Vol. 6, No. 6, 1969, pp. 481-488.

¹⁵Piereson, B. L., "Sequential Quadratic Programming and Its Use in Optimal Control Comparisons," *Optimal Control Theory and Economic Analysis 3*, edited by G. Feichtinger, North-Holland, Amsterdam, 1988,

pp. 175-193.

¹⁶Piereson, B. L., and Ong, S. Y., "Minimum-Fuel Aircraft Transition Trajectories," *Mathematical and Computer Modelling*, Vol. 12, No. 8, 1989, pp. 925-934.

¹⁷Pouliot, M. R., "CONOPT2: A Rapidly Convergent Constrained Trajectory Optimization Program for TRAJEX," General Dynamics, Convair Div., Rept. GDC-SP-82-008, San Diego, CA, 1982.

¹⁸Ong, S. Y., "A Model Comparison of a Supersonic Aircraft Minimum Time-to-Climb Problem," M.S. Thesis, Dept. of Aerospace Engineering, Iowa State Univ., Ames, IA, May 1986.

Notice to Authors and Subscribers:

AIAA produces on a quarterly basis a CD-ROM of all *AIAA Journal* papers accepted for publication. These papers will not be subject to the same paper- and issue-length restrictions as the print versions, and they will be prepared for electronic circulation as soon as they are accepted by the Associate Editor.

AIAA Journal on CD-ROM

This new product is not simply an alternative medium to distribute the *AIAA Journal*.

- Research results will be disseminated throughout the engineering and scientific communities much more quickly than in the past.
- The CD-ROM version will contain fully searchable text, as well as an index to all *AIAA journals*.
- Authors may describe their methods and results more extensively in an addendum because there are no space limitations.

The printed journal will continue to satisfy authors who want to see their papers "published" in a traditional sense. Papers still will be subject to length limitations in the printed version, but they will be enhanced by the inclusion of references to any additional material that is available on the CD-ROM.

Authors who submit papers to the *AIAA Journal* will be provided additional CD-ROM instructions by the Associate Editor.

If you would like more information about how to order this exciting new product, send your name and address to:



American Institute of
Aeronautics and Astronautics

AIAA Customer Service
1801 Alexander Bell Drive, Suite 500
Reston, VA 22091
Phone: 703/264-7500 FAX: 703/264-7551
<http://www.aiaa.org>

